Inorg. Chem. **2008**, *47*, 2205−2211

Chlorine Dioxide Oxidation of Dihydronicotinamide Adenine Dinucleotide (NADH)

Ekaterina V. Bakhmutova-Albert,[†] Dale W. Margerum,[*,†] Jameson G. Auer,[‡] and Bruce M. Applegate[‡]

Department of Chemistry, Purdue University, West Lafayette, Indiana 47907-2084, and Department of Food Science, Purdue University, West Lafayette, Indiana 47909-2009

Received September 25, 2007

The oxidation of dihydronicotinamide adenine dinucleotide (NADH) by chlorine dioxide in phosphate buffered solutions (pH 6–8) is very rapid with a second-order rate constant of 3.9×10^6 M^{-1} s^{-1} at 24.6 °C. The overall reaction stoichiometry is $2ClO_2^{\bullet}$ per NADH. In contrast to many oxidants where NADH reacts by hydride transfer, the proposed mechanism is a rate-limiting transfer of an electron from NADH to $ClO_2^{\bullet}$. Subsequent sequential fast reactions with H^+ transfer to H_2O and transfer of an electron to a second $ClO_2^{\bullet}$ give $2ClO_2^-$, H_3O^+, and NAD^+ as products. The electrode potential of 0.936 V for the $ClO_2^{\bullet}/ClO_2^-$ couple is so large that even 0.1 M of added ClO_2^- (a 10^3 excess over the initial $ClO_2^{\bullet}$ concentration) fails to suppress the reaction rate.

Introduction

Chlorine dioxide exists as a stable free radical and is a very reactive species. It is known for its antibacterial and antiviral properties.[1–6] It is effective against some parasites and has gained acceptance for use in drinking water treatment.[4] Gaseous $ClO_2^{\bullet}$ has been applied in the chemosterilization and disinfection of biological warfare agents such as anthrax.[4,7–9] Due to the oxidizing ability of chlorine dioxide ($E^0 = 0.936$ V),[10] its reactions with biological substrates are currently a subject of extensive research. It has recently been shown that chlorine dioxide reacts rapidly with tyrosine[11] and cysteine[12] as well nucleotides such as guanosine monophosphate (5′-GMP).[13] In these cases, the reaction occurs via an *electron transfer*, which plays a crucial role in many biological systems.

One of the most important biological redox reactions is the conversion of dihydronicotinamide adenine dinucleotide (NADH) to its oxidized form (NAD^+). For example, in the mitochondrial electron-transport chain, NADH functions as an energy-rich electron-transfer coenzyme and participates in ATP synthesis.[14] The NADH/NAD^+ redox couple acts as a source or acceptor of two electrons and one proton with an overall reaction of hydride transfer. The biological importance of NADH has stimulated many studies of the oxidation of NADH and its analogues. It has been established that, depending on the oxidant, the reaction may occur via one-step *hydride transfer* (H^-), by *hydrogen-atom transfer* ($H^{\bullet}-e^-$), or by sequential *electron–proton–electron transfer* ($e^- - H^+ - e^-$).[15–28] Organic oxidants such as quinones and some tetrazines tend to initiate the *hydride-transfer* pathway.

* Author to whom correspondence should be addressed. E-mail: margerum@purdue.edu.
† Department of Chemistry.
‡ Department of Food Science.

(1) Noss, C. I.; Hauchman, F. S.; Oliviere, V. P. *Water Res.* **1986**, *20*, 351–356.
(2) Masschelein, W. J.; Rice, R. G. *Chlorine Dioxide: Chemistry and Environmental Impact of Oxychlorine Compounds*; Ann Arbor Science: Ann Arbor, 1979.
(3) Neta, P.; Huie, R. E.; Ross, A. B. *J. Phys. Chem. Ref. Data* **1988**, *17*, 1027–1038.
(4) Gordon, G.; Rosenblatt, A. A. *Ozone: Sci. Eng.* **2005**, *27*, 203–207.
(5) Thurston-Enriquez, J. A.; Haas, C. N.; Jacangelo, J.; Gebra, C. P. *Appl. Environ. Microbiol.* **2005**, *71*, 3100–3105.
(6) Yuk, H.-G.; Bartz, J. A.; Schneider, K. R. *J. Food Sci.* **2006**, *71*, M95–M99.
(7) (a) Rosenblatt, D. H.; Rosenblatt, A. A.; Knapp, J. E. PCT Int. Appl. WO8401507, 1984. (b) Rosenblatt, D. H.; Rosenblatt, A. A.; Knapp, J. E. Eur. Pat. Appl. EP0159660, 1985.
(8) Rosenblatt, A. A.; Mcwhorter, T. E. PCT Int. Appl. WO03059401, 2003.
(9) Beuchat, L. R.; Pettigrew, C. A.; Tremblay, M. E.; Rosele, B. J.; Scouten, A. J. *J. Ind. Microbiol. Biotechnol.* **2005**, *32*, 301–308.
(10) Troitskaya, N. V.; Mishchenko, K. P.; Flis, I. E. *Russ. J. Phys. Chem.* **1958**, *33*, 77.
(11) Napolitano, M. J.; Green, B. J.; Nicoson, J. S.; Margerum, D. W. *Chem. Res. Toxicol.* **2005**, *18*, 501–508.
(12) Ison, A.; Odeh, I. N.; Margerum, D. W. *Inorg. Chem.* **2006**, *45*, 8768–8775.
(13) Napolitano, M. J.; Stewart, D. J.; Margerum, D. W. *Chem. Res. Toxicol.* **2006**, *19*, 1451–1458.
(14) Voet D.; Voet, J. G. *Biochemistry*, 3rd ed.; J. Wiley & Sons: Hoboken, NJ, 2004; Chapter 16.
(15) Matsuo, T.; Mayer, J. M. *Inorg. Chem.* **2005**, *44*, 2150–2158.
(16) (a) Eisner, U.; Kuthan, J. *Chem. Rev.* **1972**, *72*, 1–42. (b) Stout, D. M.; Meyers, A. I. *Chem. Rev.* **1982**, *82*, 223–243.
(17) Fukuzumi, S.; Itoh, S. *Antioxid. Redox Signaling* **2001**, *3*, 807–824.

10.1021/ic7019022 CCC: $40.75
Published on Web 02/16/2008

For example, the oxidation of NADH by benzo- and naphthaquinones most likely occurs with *hydride transfer*, while the sequential ($e^- - H^+ - e^-$) pathway is ruled out.[23] A single *hydride-transfer* mechanism is suggested for oxidation of a NADH analogue, substituted BNAH.[21f] At the same time, the change of pathways from one to another also is possible if different tetrazine substituents are used. Yuasa and Fukuzumi demonstrated that the mechanism of $AcrH_2$ (NADH analogue) oxidation changes from a *hydride transfer* to an *electron transfer* upon substitution of diphenyltetrazine by dipyridyltetrazine.[19] The deuterium substitution of $AcrH_2$ by $AcrD_2$ similarly affects the mechanism.[20]

Some studies have suggested that strong one-electron inorganic oxidants can initiate a sequential *electron-transfer* pathway.[24a,25] Recent observation of the $NADH^{\bullet+}$ radical cation and its deprotonated form ($NAD^{\bullet}$) in the reaction of NADH with the dibromide radical ($Br_2^{\bullet-}$) has confirmed the involvement of an *electron-transfer* step in this oxidation.[28,29]

In the present work, we report the rapid oxidation of NADH by $ClO_2^{\bullet}$ with an evaluation of the stoichiometry, kinetics, and the mechanism.

Experimental Section

Materials. β-NADH (Sigma) was kept under argon and used without further purification. NADH stock solutions were freshly prepared and utilized on the day of each experiment. Chlorine dioxide solutions were prepared as previously described.[30] The solutions were protected from light and stored in a refrigerator. Concentrations of NADH and $ClO_2^{\bullet}$ in each sample were determined spectrophotometrically ($\lambda = 340$ and 359 nm), on the basis of ϵ_{340}^{NADH} (6220 M^{-1} cm^{-1})[31,32] and $\epsilon_{359}^{ClO_2}$ (1230 M^{-1} cm^{-1}),[30] respectively (Table 1). Sodium chlorite for kinetic experiments was recrystallized,[33] and stock solutions were standardized spectrophotometrically at 260 nm ($\epsilon_{260}^{ClO_2^-} = 154$ M^{-1} cm^{-1}).[30] All solutions were prepared with distilled–deionized water.

Table 1. Molar Absorptivities of NADH, $ClO_2^{\bullet}$, and NAD^+ in Aqueous Solutions

	molar absorptivity, ϵ (M^{-1} cm^{-1})		
λ (nm)	NADH	$ClO_2^{\bullet}$[a]	NAD^+
260	14100[b]	45	17400[b]
340	6220[b]	1100	57[c]
359		1230[d]	
400		568	
410		401	

[a] Determined experimentally unless otherwise indicated. [b] ϵ_{260}^{NADH}, ϵ_{340}^{NADH}, and ϵ_{260}^{NAD+} are obtained from ref 30. [c] ϵ_{340}^{NAD+} is taken from Figure 2a of ref 34. [d] $\epsilon_{359}^{ClO_2}$ is obtained from ref 29.

Methods. The reactions were carried out at three temperatures: 3.1, 9.8, and 24.6 °C (± 0.1 °C). The pH was maintained in the range of 6.0−8.2 with 0.005 or 0.05 M phosphate buffer that produced the ionic strength in the 0.10−0.15 M range. An Orion model 720A digital pH meter equipped with a Corning combination of electrodes was used for pH measurements that were corrected to give $p[H^+]$ values [i.e., $-\log(H^+$ concentration)], based on electrode calibrations at an ionic strength of 0.10 M ($p[H^+] = 0.9816 \times pH + 0.057$).

UV spectra (200–500 nm) of the initial compounds (NADH, $ClO_2^{\bullet}$, and $NaClO_2$) and NADH−$ClO_2^{\bullet}$ mixtures after reaction completion were recorded with a Lambda 9 Perkin-Elmer UV–vis spectrophotometer (path lengths of 0.1 and 1.0 cm). The molar absorptivities of NADH, $ClO_2^{\bullet}$, and NAD^+ used in this work are given in Table 1. Variable-temperature kinetic measurements were performed on an Applied Photophysics Stopped-flow SX.18 MV (APPSF) with a path length of 0.962 cm at 340 and 400 or 410 nm. Ion exchange chromatographic analysis was carried out on a Dionex DX 500 chromatographic system with a Dionex ED40 electrochemical detector. A Dionex Ion-Pac AS9-HC column was used for separations with a 9.0 mM sodium carbonate mobile phase. The analysis was performed for mixtures with initial concentration ratios of $[ClO_2^{\bullet}]_i/[NADH]_i > 2$. Any excess of unreacted $ClO_2^{\bullet}$ was removed by bubbling argon through the cold sample for about 3–5 min. UV spectra (200–500 nm) of the same samples were recorded to determine the concentration of reagents left after reaction completion.

Results and Discussion

The oxidation of NADH by chlorine dioxide was studied at a variety of reagent ratios ($[ClO_2^{\bullet}]_i/[NADH]_i = 0.49–5.97$). The pH ($p[H^+] = 7.2 \pm 0.1$) was maintained close to physiological conditions to avoid possible acid-catalyzed hydration of NADH.[34] The products formed were detected by UV–vis spectroscopy and by ion chromatography.

Reaction Stoichiometry. The UV spectrum of the NADH solution exhibits two maxima: one (260 nm) is due to the adenine ring, and the other (340 nm) arises from the reduced nicotinamide ring[35] (Figure 1, spectrum 1). The stepwise addition of chlorine dioxide from equimolar levels to 2-fold excess leads to a decrease and a subsequent loss of the

(18) (a) Fukuzumi, S.; Inada, O.; Suenobu, T. *J. Am. Chem. Soc.* **2002**, *124*, 14538–14539. (b) Fukuzumi, S.; Inada, O.; Suenobu, T. *J. Am. Chem. Soc.* **2003**, *125*, 4808–4816.
(19) Yuasa, J.; Fukuzumi, S. *J. Am. Chem. Soc.* **2006**, *128*, 14281–14292.
(20) Yuasa, J.; Yamada, S.; Fukuzumi, S. *J. Am. Chem. Soc.* **2006**, *128*, 14938–14948.
(21) (a) Zhu, X.-Q.; Yang, Y.; Zhang, M.; Cheng, J.-P. *J. Am. Chem. Soc.* **2003**, *125*, 15298–15299. (b) Zhu, X.-Q.; Cao, L.; Liu, Y.; Yang, Y.; Lu, J.-Y.; Wang, J.-S.; Cheng, J.-P. *Chem.—Eur. J.* **2003**, *9*, 3937–3945. (c) Zhu, X.-Q.; Li, H.-R.; Li, Q.; Ai, T.; Lu, J.-Y.; Yang, Y.; Cheng, J.-P. *Chem.—Eur. J.* **2003**, *9*, 871–880. (d) Cheng, J.-P.; Lu, Y.; Zhu, X.; Mu, L. *J. Org. Chem.* **1998**, *63*, 6108–6114. (e) Cheng, J.-P.; Handoo, K. L.; Xue, J.; Parker, V. D. *J. Org. Chem.* **1993**, *58*, 5050–5054. (f) Zhu, X.-Q.; Zhang, J.-Y.; Cheng, J.-P. *J. Org. Chem.* **2006**, *71*, 7007–7015.
(22) Carlson, B. W.; Miller, L. L. *J. Am. Chem. Soc.* **1985**, *107*, 479–485.
(23) Scherbak, N.; Strid, A.; Eriksson, L. A. *Chem. Phys. Lett.* **2005**, *414*, 243–247.
(24) (a) Land, E. J.; Swallow, A. J. *Biochim. Biophys. Acta* **1971**, *234*, 34–42. (b) Land, E. J.; Swallow, A. J. *Biochim. Biophys. Acta* **1968**, *162*, 327.
(25) (a) Grodkowski, J.; Neta, P.; Carlson, B. W.; Miller, L. L. *J. Chem. Phys.* **1983**, *87*, 3135–3138. (b) Hore, P. J.; Volbeda, A.; Dijkstra, K.; Kaptein, R. *J. Am. Chem. Soc.* **1982**, *104*, 6262–6267.
(26) Hore, P. J.; Volbeda, A.; Dijkstra, K.; Kaptein, R. *J. Am. Chem. Soc.* **1982**, *104*, 6262–6267.
(27) Takahashi, N.; Shinno, T.; Tackikawa, M.; Yuzawa, T.; Takahashi, H. *J. Raman Spectrosc.* **2006**, *37*, 283–290.
(28) Zielonka, J.; Marcinec, A.; Adamus, J.; Gebicki, J. *J. Phys. Chem. A* **2003**, *107*, 9860–9864.
(29) Gebicki, J.; Marcinec, A.; Zielonka, J. *Acc. Chem. Res.* **2004**, *37*, 379–386.
(30) Furman, C. S.; Margerum, D. W. *Inorg. Chem.* **1998**, *37*, 4321–4327.
(31) Horecker, B. L.; Kornberg, A. *J. Biol. Chem.* **1948**, *175*, 385–390.
(32) Haid, E.; Lehmann, P.; Ziegenhorn, J. *Clin. Chem.* **1975**, *21*, 884–887.
(33) Jia, Z.; Margerum, D. W.; Francisco, J. S. *Inorg. Chem.* **2000**, *39*, 2614–2620.
(34) Achenson, S. A.; Kirkman, H. N.; Wolfenden, R. *Biochemistry* **1988**, *27*, 7371–7375.
(35) Malcolm, A. D. B. *Methods Enzymol.* **1980**, *66*, 8–11.

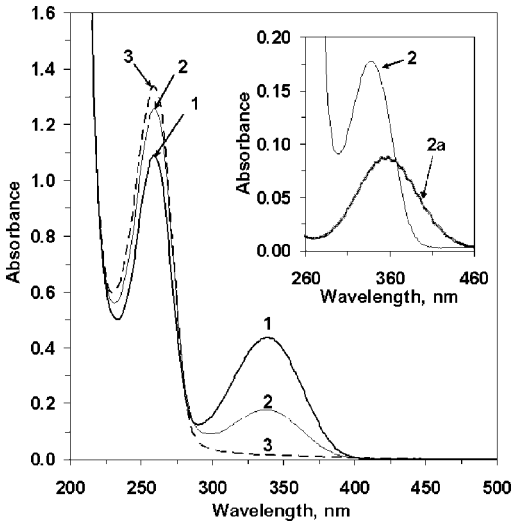

Figure 1. Selected UV spectra of NADH−$ClO_2^{\bullet}$ reaction mixtures, recorded at 25 °C and p[H^+] 7.2 ± 0.1, with a path length of 1.0 cm. (1) NADH (7.10×10^{-5} M) without $ClO_2^{\bullet}$; (2) NADH (7.10×10^{-5} M) mixed with $ClO_2^{\bullet}$ (7.12×10^{-5} M); (3) NADH (7.10×10^{-5} M) mixed with $ClO_2^{\bullet}$ (1.44×10^{-4} M). Inset: (2) NADH (7.10×10^{-5} M) mixed with $ClO_2^{\bullet}$ (7.12×10^{-5} M); (2a) free $ClO_2^{\bullet}$ (7.12×10^{-5} M). $ClO_2^{\bullet}$ shows appreciable absorbance at 410 nm that is not present in the NADH/$ClO_2^{\bullet}$ mixture.

absorption band at 340 nm. On the other hand, the absorbance at 260 nm increases in its intensity (Figure 1, spectra 2 and 3). These changes agree with the conversion of NADH to NAD^+. The UV spectrum of NAD^+ has a single absorption band with $\lambda_{max} = 260$ nm.[27] It should be noted that approximately half of the NADH is reacted, and chlorine dioxide is no longer observed in the UV spectrum for a 1:1 reagent ratio (Figure 1, spectrum 2). Both NADH and chlorine dioxide react to completion at a 2-fold excess of $ClO_2^{\bullet}$ (Figure 1, spectrum 3). The disappearance of $ClO_2^{\bullet}$ ($\lambda_{max} = 359$ nm) was monitored at 410 nm where the molar absorptivity of $ClO_2^{\bullet}$ is significant (401 M^{-1} cm^{-1}, Table 1) and NADH does not absorb. Comparison of the UV spectrum of free $ClO_2^{\bullet}$ (Figure 1, inset) with spectra of NADH mixed with $ClO_2^{\bullet}$ (Figure 1, spectra 2 and 3) demonstrates that chlorine dioxide is consumed in both cases. The results show that the [$ClO_2^{\bullet}$]/[NADH] stoichiometric ratio is 2.0.

It has previously been shown that chlorine dioxide can oxidize organic species with the formation of a chlorite ion (ClO_2^-).[11–13] For example, the oxidation of N-acetyltyrosine, tyrosine,[11] and guanosine[13] produces ClO_2^- in the first step. During cysteine oxidation, $ClO_2^{\bullet}$ is initially reduced to ClO_2^-, then to HOCl, and subsequently to Cl^-.[12] To analyze the products of chlorine dioxide reduction in the present work and to confirm the stoichiometry of the reaction by an independent method, an ion exchange chromatographic analysis was performed for the NADH/$ClO_2^{\bullet}$ reaction mixtures. A series of solutions was prepared where $[ClO_2^{\bullet}]_i$ was constant and $[NADH]_i$ was gradually increased in each solution. For simplicity, only samples with $[ClO_2^{\bullet}]_i/[NADH]_i > 2$ were used to ensure that all NADH was consumed by $ClO_2^{\bullet}$ ($[NADH]_r$). The main species detected by ion chromatography is ClO_2^-. [ClO_2^-] increases (0.1−0.15 mM) as expected with a rise in $[NADH]_i$. Although background Cl^- is also observed, its concentration (0.014 mM) is constant for all samples. Moreover, similar amounts of Cl^- are

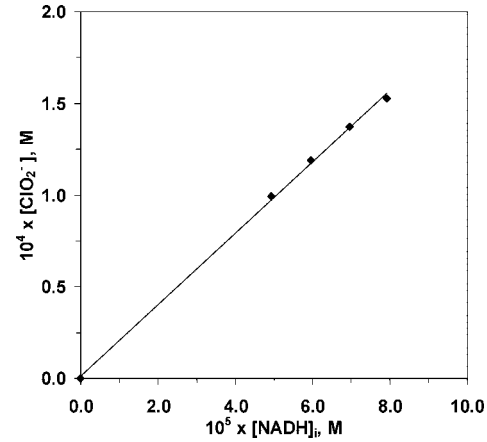

Figure 2. Concentration of chlorite ions formed in the reaction of NADH with $ClO_2^{\bullet}$ as determined by ion chromatography (25 °C and p[H^+] 7.2 ± 0.1). $[ClO_2^{\bullet}]_i$ is 1.84×10^{-4} M, and the ratio of $[ClO_2^{\bullet}]_i/[NADH]_i$ varies from 3.7 to 2.3. The slope equals 1.95 ± 0.04, which corresponds to the reaction stoichiometry.

Scheme 1. The Overall Reaction of NADH with $ClO_2^{\bullet}$

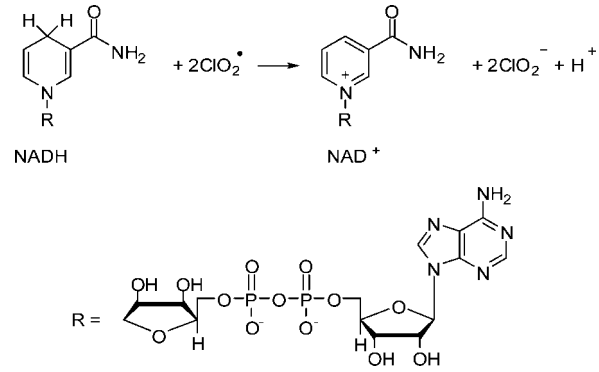

detected in the chlorine dioxide solution itself. Therefore, Cl^- is not produced by the reaction, while ClO_2^- is definitely the result of NADH oxidation by chlorine dioxide.

Because ClO_2^- is shown to be a single product of the NADH−$ClO_2^{\bullet}$ reaction, the stoichiometry can be determined from the $[ClO_2^-]/[NADH]_r$ ratio where [ClO_2^-] is obtained from ion chromatography data and $[NADH]_r$ is equivalent to $[NADH]_i$ under the conditions of the experiment. Figure 2 shows [ClO_2^-] formed as a linear function of NADH initial concentration ($[NADH]_i$). The slope (1.95 ± 0.04) corresponds to the stoichiometry of the reaction, which is in agreement with the stoichiometry proposed from UV spectra (Figure 1). Thus, 2 mol of chlorine dioxide are needed for conversion of 1 mol of NADH (Scheme 1).

Analysis of UV spectra (200–500 nm) shows that NADH is oxidized to give NAD^+ as a product. The UV spectra were recorded for a variety of reagent ratios, but always with $[ClO_2^{\bullet}]_i/[NADH]_i > 2$, so that all NADH was consumed. Therefore, NADH ($\lambda_{max} = 260$ and 340 nm) does not contribute to the spectrum of NAD^+ ($\lambda_{max} = 260$ nm). The decrease of the $ClO_2^{\bullet}$ absorption band (359 nm) and the growth of the NAD^+ band (260 nm) upon NADH addition occur with an isobestic point at 300 nm (Figure 3). The concentration of NAD^+ formed is determined from the absorption band at 260 nm (A_{260}) that is measured for each reagent ratio with a cell path length of 1.0 cm. The A_{260}

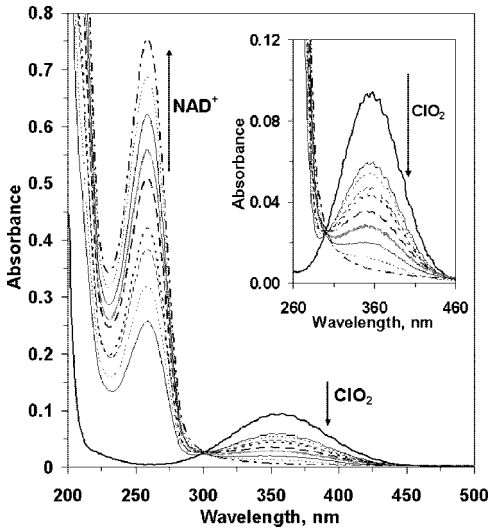

Figure 3. The UV spectra of $ClO_2^{\bullet}$ and NADH−$ClO_2^{\bullet}$ reaction mixtures, recorded at 25 °C and p[H^+] 7.2 ± 0.1, with a path length of 1.0 cm. $[ClO_2^{\bullet}]_i$ is constant throughout the experiment (7.63×10^{-5} M); $[NADH]_i$ is gradually increased in each sample. $[ClO_2^{\bullet}]_i/[NADH]_i$ varies in a 2.2−5.7 range, which ensures that all NADH is consumed by $ClO_2^{\bullet}$ ($[NADH]_i = [NADH]_r$). The $ClO_2^{\bullet}$ absorption band (359 nm) decreases with increasing $[NADH]_i$, while the NAD^+ absorbance (260 nm) increases.

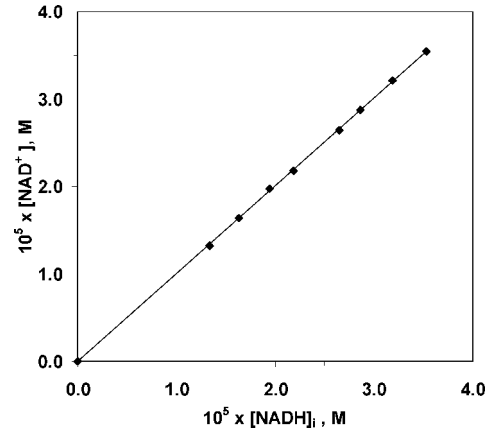

Figure 4. The formation of NAD^+, depending on the initial concentration of NADH. $[NAD^+]$ is determined by eq 1, The data are obtained from UV spectra of $ClO_2^{\bullet}$−NADH reaction mixtures, recorded for $[ClO_2^{\bullet}]_i/[NADH]_i$ ratios of 2.2−5.7 (25 °C, p[H^+] 7.2 ± 0.1, 1.0 cm path length). Because $[ClO_2^{\bullet}]_i/[NADH]_i > 2$, the amount of NADH reacted with $ClO_2^{\bullet}$ is equal to the NADH initial concentration ($[NADH]_r = [NADH]_i$). The slope, or $[NAD^+]/[NADH]_i$ ratio, is 1.00 ± 0.02.

values include the absorbance of NAD^+, the absorbance of $ClO_2^{\bullet}$ left after the reaction, and the absorbance of ClO_2^- formed. Hence, $[NAD^+]$ can be obtained from eq 1, where $[ClO_2^{\bullet}]_i$ and $[ClO_2^{\bullet}]_{left}$ are concentrations of the initial $ClO_2^{\bullet}$ and $ClO_2^{\bullet}$ that is not consumed. $[ClO_2^{\bullet}]_{left}$ is determined from the UV spectra at 359 nm (Figure 3).The molar extinction coefficients of $ClO_2^{\bullet}$, ClO_2^-, and NAD^+ at 260 nm ($\epsilon_{260}^{ClO_2}$, $\epsilon_{260}^{ClO_2^-}$, and ϵ_{260}^{NAD+}) are given in Table 1, and the cell path length is 1.0 cm.

$$[NAD^+] = \frac{A_{260} - [ClO_2^{\bullet}]_{left}(\epsilon_{260}^{ClO_2^{\bullet}} - \epsilon_{260}^{ClO_2^-}) - [ClO_2^{\bullet}]_i \epsilon_{260}^{ClO_2^-}}{\epsilon_{260}^{NAD^+}} \quad (1)$$

Under the experimental conditions used, all of the NADH is consumed by $ClO_2^{\bullet}$. Plotting $[NAD^+]$ versus $[NADH]_i$ gives a linear dependence (Figure 4). The slope represented by the $[NAD^+]/[NADH]_i$ ratio is 1.00 ± 0.02. This confirms that NADH reacts with $ClO_2^{\bullet}$ to give NAD^+ as the only product of the oxidation ($[NADH]_r = [NAD^+]$).

Kinetics. The reaction kinetics were followed by stopped-flow methods with single-wavelength detection. Overlapping absorption bands of NADH ($\lambda_{max} = 340$ nm, $\epsilon_{340}^{NADH} = 6220$ M^{-1} cm^{-1}) and chlorine dioxide ($\lambda_{max} = 359$ nm, $\epsilon_{359}^{ClO_2} = 1230$ M^{-1} cm^{-1}) complicate the kinetics observation and make pseudofirst-order conditions (significant excess of one of the reagents) impossible. Therefore, the absorbance of one of the reactants must be corrected for the presence of the other. In accordance with UV spectra, NADH does not absorb at wavelengths higher than 400 nm (Figure 1, spectrum 1), while the molar absorptivity of $ClO_2^{\bullet}$ is significant in this region ($\epsilon_{410}^{ClO_2} = 401$ M^{-1} cm^{-1}). In order to make appropriate corrections, both NADH (340 nm) and $ClO_2^{\bullet}$ losses (410 nm) were monitored with the $[ClO_2^{\bullet}]_i/[NADH]_i$ ratio varied from 0.5 to 5.9. The absorbance of NADH (A_{340}^{NADH}) was then corrected for the contribution of $ClO_2^{\bullet}$ by eq 2, where A_{340} is the absorbance measured at t time; $[NADH]_t$ is the concentration of NADH at each t that is not reacted; ϵ_{340}^{NADH}, ϵ_{340}^{NAD+},[36] $\epsilon_{340}^{ClO_2}$, and $\epsilon_{410}^{ClO_2}$ are molar absorptivities of NADH, NAD^+, and $ClO_2^{\bullet}$ (Table 1); and l is the path length (0.962 cm). The $ClO_2^{\bullet}$ contribution is determined from independently measured kinetic curves at 410 nm ($\epsilon_{340}^{ClO_2} A_{410}^{ClO_2}/\epsilon_{410}^{ClO_2}$). The NAD^+ contribution is defined as NADH reacted with $ClO_2^{\bullet}$ [$l\epsilon_{340}^{NAD+}([NADH]_i - [NADH]_t)$]. To construct the NADH kinetic curve, such corrections are performed separately for each time t.

$$A_{340}^{NADH} = l\epsilon_{340}^{NADH}[NADH]_t = \frac{\epsilon_{340}^{NADH}}{\epsilon_{340}^{NADH} - \epsilon_{340}^{NADH^+}} \times \left(A_{340} - \frac{A_{410}^{ClO_2^{\bullet}}}{\epsilon_{410}^{ClO_2^{\bullet}}} \epsilon_{340}^{ClO_2^{\bullet}} - l\epsilon_{340}^{NAD^+}[NADH]_i \right) \quad (2)$$

Note that the corrections given in eq 2 are made independently of stoichiometric assumptions and are based on absorbance measurements and extinction coefficients, without additional consideration of the reactant concentration gradients due to mixing. Other approaches to fast second-order reactions measured by stopped-flow techniques have been recommended,[37–40] where methods are suggested to correct concentration gradients and programs are developed for the correction. As noted by Meagher et al.,[37] a standard second-order treatment that ignores concentration gradients yields

(36) Reisbig, R. R.; Woody, R. W. *Biochemistry* **1978**, *17*, 1974–1984.
(37) Meagher, N. E.; Rorabacher, D. B. *J. Phys. Chem.* **1994**, *98*, 12590–12593.
(38) Dunn, B. C.; Meagher, N. E.; Rorabacher, D. B. *J. Phys. Chem.* **1996**, *100*, 16925–16933.
(39) Peintler, G.; Horvath, A. K.; Kortvelyesi, T.; Nagypal, I. *Phys. Chem. Chem. Phys.* **2000**, *2*, 2575–2586.
(40) (a) Horvath, A. K.; Istvan, N. *J. Phys. Chem. A* **1998**, *102*, 7267–7272. (b) Horvath, A. K.; Istvan, N. *J. Phys. Chem. A* **2006**, *110*, 4753–4758.

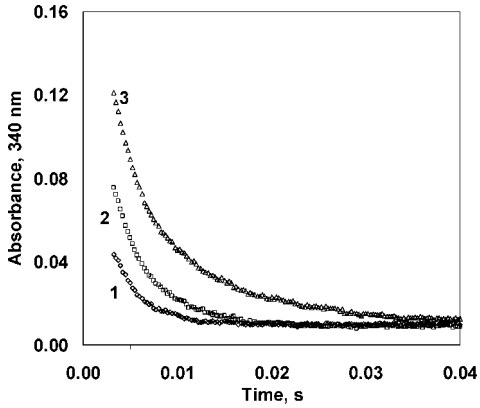

Figure 5. Selected kinetic traces of NADH oxidation at 24.6 °C and p[H$^+$] 7.2 ± 0.1. The absorbance of NADH at 340 nm is corrected for the contribution of $ClO_2^\bullet$ (kinetic measurements at 410 nm) and NAD^+ (eq 2). $[ClO_2^\bullet]_i = 9.01 \times 10^{-5}$ M; $[NADH]_i$ is (1) 1.51×10^{-5} M; (2) 2.72×10^{-5} M; and (3) 4.01×10^{-5} M.

Table 2. Observed Second-Order Rate Constants for the Loss of NADH (k_{obs}^{NADH}) and for the Loss of $ClO_2^\bullet$ ($k'_{obs}^{ClO_2}$) from 3.1 to 24.6 °C[a]

t, °C	$10^{-6} \times k_{obs}^{NADH}$ (M^{-1} s^{-1})	$10^{-6} \times k'_{obs}^{ClO_2^\bullet}$ (M^{-1} s^{-1})
3.1	1.8 ± 0.1	3.6 ± 0.3
9.8	2.6 ± 0.2	5.4 ± 0.4
24.6	3.9 ± 0.5[b]	7.6 ± 0.6[b]
	4.1 ± 0.5[c]	8.0 ± 1.0[c]
	4.0 ± 0.2[d]	8.4 ± 1.2[d]
	3.5 ± 0.4[e]	7.8 ± 1.9[e]

[a] $[NADH]_i$ is in the range of 0.02–0.13 mM; $[ClO_2^\bullet]_i$ is varied between 0.06 and 0.15 mM. [b] p[H$^+$] = 7.2, 0.05 M phosphate buffer. [c] p[H$^+$] = 6.0, 0.05 M phosphate buffer. [d] p[H$^+$] = 8.0, 0.05 M phosphate buffer. [e] p[H$^+$] = 8.2, 0.005 M phosphate buffer.

rate constant values that are virtually identical to those obtained when the concentration gradient is taken into account. Hence, with the limited data available to us in the present system, we have not attempted additional corrections. Selected kinetic traces of NADH oxidation are presented in Figure 5. The reaction of NADH with chlorine dioxide occurs rapidly and is nearly complete in 30 ms. In fact, the reaction is so fast that the time needed for half of the $[NADH]_i$ to react is less than 3.3 ms at 24.6 °C, which is approximately the mixing time of the instrument.

Because the pseudo-first-order conditions are not used, both reactants affect the rate. Therefore, the changes of both NADH and $ClO_2^\bullet$ concentrations with time were considered. The instantaneous rates were determined from kinetic curves as slopes taken for overlapping sets of three measurements at an early stage of the reaction (3.5–4.5 ms). To obtain second-order rate constants, the instantaneous rates were then divided by concentrations of NADH and $ClO_2^\bullet$ at the time where the rates were measured. Both [NADH] and $[ClO_2^\bullet]$ are based on experimental results and are either corrected with eq 2 (for NADH) or determined directly from the absorbance decay at 410 nm (for $ClO_2^\bullet$). The procedure was repeated for a number of $[ClO_2^\bullet]_i/[NADH]_i$ ratios (0.5–5.9). The average observed rate constants obtained from NADH (k_{obs}^{NADH}, M^{-1} s^{-1}) and ClO_2 ($k'_{obs}^{ClO_2}$, M^{-1} s^{-1}) losses are summarized in Table 2.

As demonstrated by ion exchange chromatography, 1 mol of NADH reacts with 2 mol of $ClO_2^\bullet$ to give $2ClO_2^-$ (Scheme 1). The rate expression for the reaction with this stoichiometry is given in eq 3, where k_{obs}^{NADH} (M^{-1} s^{-1}) is the observed rate constant, obtained for NADH decay.

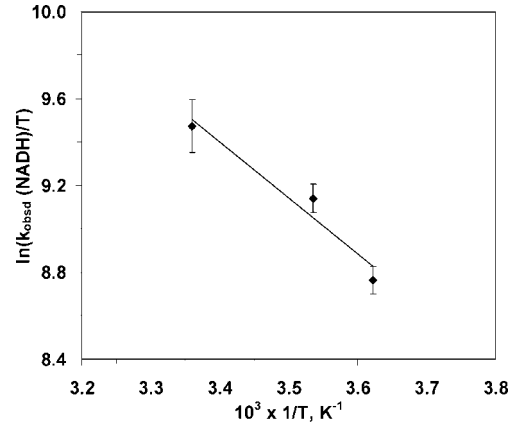

Figure 6. Temperature profile of NADH reaction with $ClO_2^\bullet$ for 3.1, 9.8, and 24.6 °C and p[H$^+$] 7.1. The enthalpy of activation ($\Delta H^\ddagger = 5 \pm 1$ kcal mol^{-1}) is determined from the slope. The entropy of activation ($\Delta S^\ddagger = -11 \pm 4$ cal mol^{-1} K^{-1}) is estimated from the intercept. The vertical bars are the standard deviation of $\ln(k_{obs}^{NADH}/T)$.

$$-\frac{d[NADH]}{dt} = \frac{1}{2}\frac{d[ClO_2^\bullet]}{dt} = k_{obs}^{NADH}[NADH][ClO_2^\bullet] \quad (3)$$

Therefore, the rate constant, determined from $ClO_2^\bullet$ decay, is expected to be twice that obtained from NADH decay ($k'_{obs}^{ClO_2} = 2k_{obs}^{NADH}$). Indeed, the average ratio of $k'_{obs}^{ClO_2}/k_{obs}^{NADH}$ is 2.01 ± 0.14. This independently confirms the stoichiometry and supports the ion chromatographic data that give a stoichiometry of 1.95 ± 0.04. It also demonstrates the validity of A_{340}^{NADH} corrections with the use of eq 2.

Kinetic measurements were performed at lower temperatures as well. The rates decrease with decreasing temperature (Table 2). However, the reaction is still very rapid even with a 20 °C temperature decrease (the time necessary for the reaction of half of the $[NADH]_i$ goes from less than 3.3 up to 5.8 ms). For example, k_{obs}^{NADH}, obtained at 3.1 °C, is 1.8×10^6 M^{-1} s^{-1}, which is approximately 2 times smaller than that determined at 24.6 °C (3.9×10^6 M^{-1} s^{-1}; Table 2). This corresponds to a low activation energy. The enthalpy and entropy of activation are estimated from the transition state equation (eq 4), where k_{obs}^{NADH} (M^{-1} s^{-1}) is the observed rate constant for the loss of NADH.

$$\ln\frac{k_{obs}^{NADH}}{T} = \ln\frac{k_B}{h} + \frac{\Delta S^\ddagger}{R} - \frac{\Delta H^\ddagger}{RT} \quad (4)$$

Figure 6 is a plot of eq 4 where the slope × R gives $\Delta H^\ddagger = 5 \pm 1$ kcal mol^{-1}. The entropy of activation ($\Delta S^\ddagger = -11 \pm 4$ cal mol^{-1} K^{-1}), determined from the intercept, is negative.

Mechanism. It has previously been shown that the oxidation of NADH by strong one-electron inorganic oxidants such as $Br_2^{\bullet-}$, $I_2^{\bullet-}$, and $(SCN)_2^{\bullet-}$ occurs with an *electron transfer*.[24,25,27,28] The ability of the oxidants to initiate an *electron transfer* has been supported by $NAD^\bullet$ detection in pulse radiolysis studies of NADH reactions.[24,25] Recent observation of $NADH^{\bullet+}$ transient species with a subsequent formation of $NAD^\bullet$ in the oxidation by $Br_2^{\bullet-}$

Scheme 2. Proposed Mechanism of NADH Oxidation by $ClO_2^{\bullet}$ to Give NAD^+

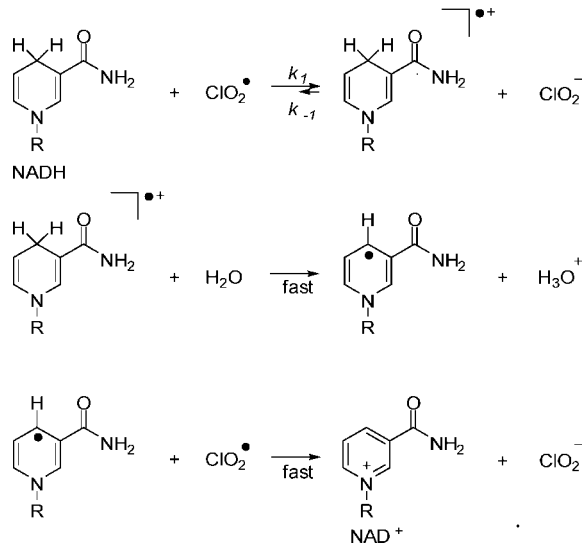

directly confirms an *electron-transfer* mechanism for NADH with several inorganic oxidant systems.[27,28] $ClO_2^{\bullet}$ is a powerful one-electron oxidant ($E^0 = 0.936$ V vs NHE) and is a free radical similar to the inorganic oxidants such as $Br_2^{\bullet-}$, $I_2^{\bullet-}$, and $(SCN)_2^{\bullet-}$. $ClO_2^{\bullet}$ is relatively stable and does not require *in situ* generation, unlike the oxidants mentioned above that have to be generated by pulse radiolysis. Chlorine dioxide rapidly oxidizes some amino acids and nucleotides, leading to a chlorite ion formation (ClO_2^-) as a result of an *electron transfer* to chlorine dioxide.[11–13] All these results and our experimental detection of ClO_2^- by ion chromatography allow us to propose Scheme 2 for NADH oxidation by $ClO_2^{\bullet}$. First, chlorine dioxide accepts one electron from NADH, to form ClO_2^- and the radical cation $NADH^{\bullet+}$. Then, the subsequent sequence of very fast deprotonation and second electron transfer proceeds with the formation of another equivalent of ClO_2^- and the final product NAD^+. This sequence can often be very rapid.[25a,27,28] For example, in the reaction of NADH with $Br_2^{\bullet-}$, $NADH^{\bullet+}$ decays in less than 1 μs (1.69 V vs NHE) with the rate constant of 3.5×10^6 s^{-1}.[25a,27,28] The rate of a second electron transfer for the $ClO_2^{\bullet}$ oxidation of guanosine is reported to be close to diffusion-controlled.[13] Therefore, in the current work, the initial transfer of an electron from NADH to $ClO_2^{\bullet}$ (Scheme 2) is considered to be the rate-determining step.

It has previously been demonstrated that the transfer of the first electron from guanosine to $ClO_2^{\bullet}$ is reversible, as shown by reaction rate suppression with ClO_2^- addition.[13] However, the addition of chlorite ions to the NADH−$ClO_2^{\bullet}$ reaction mixture does not suppress the rate of reaction (Scheme 2 and Table 3). A 10^3-fold excess of ClO_2^- ($[ClO_2^-]_i = 0.11$ M) gives the same rate constant (4.3×10^6 M^{-1} s^{-1}) as estimated previously within the experimental error [$(3.9 \pm 0.5) \times 10^6$ M^{-1} s^{-1}; Table 2]. These results show that, if any reversibility exists, it is negligible due to the rapid subsequent reactions. Therefore, the observed rate constant (k_{obs}^{NADH}) determined experimentally from NADH decay is equivalent to k_1 in Scheme 2. Hence, the rate is given by eq 5.

$$-\frac{d[NADH]}{dt} = k_1[NADH][ClO_2^{\bullet}] = k_{obs}^{NADH}[NADH][ClO_2^{\bullet}] \quad (5)$$

Variation of both pH (6–8) and the concentration of the phosphate buffer do not affect the rate (Table 2). Selected initial decays of NADH are shown in Figure 7. The slope, which represents instantaneous rate, does not change with increasing pH. It indicates that acid–base equilibrium is not involved in the rate-determining step. Carlson et al. have previously observed the independence of the rate on pH for the oxidation of NADH by the ferrocenium radical cation $[Fe(Cp)_2^{\bullet+}]$.[41] They have also found the same stoichiometry of two and suggested a similar mechanism with rate-limiting initial electron transfer. It should be emphasized, however, that the reaction of NADH with $ClO_2^{\bullet}$ ($k_1 = 3.9 \times 10^6$ M^{-1} s^{-1}) is almost 6 orders of magnitude faster than the NADH reaction with $Fe(Cp)_2^{\bullet+}$ ($k_1 = 5.41$ M^{-1} s^{-1}), which correlates with standard potentials. $E^0_{Fe(Cp)_2^{\bullet+}/Fe(Cp)_2}$ is 0.395 V at pH 7, while $E^0_{ClO_2/ClO_2^-}$ has a higher value (0.936 V[10]). Comparison of our experimental data for the NADH−$ClO_2^{\bullet}$ reaction with published results for $Fe(Cp)_2^{\bullet+}$,[41b] $Br_2^{\bullet-}$,[26] $(SCN)_2^{\bullet-}$,[26] and $I_2^{\bullet-}$[26] demonstrates that the rate constants (k^{ox}, $M^{-1}s^{-1}$) increase in the same order as the strength of oxidants (E^0, V) does. The neutral radical $ClO_2^{\bullet}$ oxidizes

(41) (a) Carlson, B. W.; Miller, L. L. *J. Am. Chem. Soc.* **1983**, *105*, 7453–7454. (b) Carlson, B. W.; Miller, L. L.; Neta, P.; Grodkowski, J. *J. Am. Chem. Soc.* **1984**, *106*, 7233–7239.

Table 3. Observed Second-Order Rate Constants for NADH Decay (k_{obs}^{NADH}) Obtained with the Addition of ClO_2^- in an Unsuccessful Attempt to Suppress the Reaction

$[ClO_2^-]$ (mM)	$[ClO_2^-]/[ClO_2^{\bullet}]_i$	$10^{-6} \times k_{obs}^{NADH}$ (M^{-1} s^{-1})[a]
0		3.9 ± 0.5
0.32	4	3.6 ± 0.3
3.52	29	3.4 ± 0.3
5.85	59	3.8 ± 0.3
12.0	120	4.0 ± 0.5
110.0	917	4.3 ± 0.1

[a] Conditions: $[NADH]_i = 0.04 - 0.06$ mM, 24.6 °C, $p[H^+] = 7.2 \pm 0.1$.

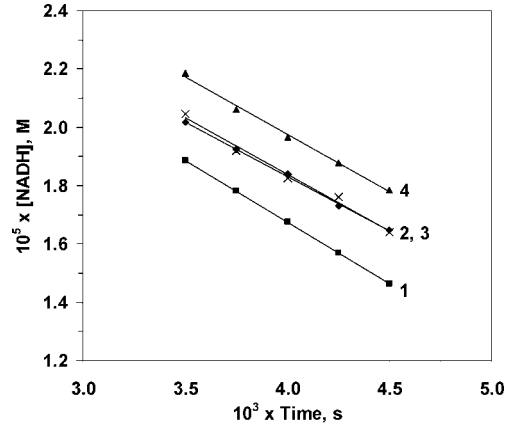

Figure 7. Rates of NADH disappearance for a variety of pH's and phosphate buffer concentrations at 24.6 °C. (1) $p[H^+]$ 7.2, 0.05 M phosphate buffer, $[NADH]_i = 5.25 \times 10^{-5}$ M, $[ClO_2^{\bullet}]_i = 1.23 \times 10^{-4}$ M; (2) $p[H^+]$ 6.0, 0.05 M phosphate buffer, $[NADH]_i = 5.24 \times 10^{-5}$ M, $[ClO_2^{\bullet}]_i = 1.10 \times 10^{-4}$ M; (3) $p[H^+]$ 8.2, 0.005 M phosphate buffer, $[NADH]_i = 5.32 \times 10^{-5}$ M, $[ClO_2^{\bullet}]_i = 1.21 \times 10^{-4}$ M; (4) $p[H^+]$ 8.0, 0.05 M phosphate buffer, $[NADH]_i = 5.32 \times 10^{-5}$ M, $[ClO_2^{\bullet}]_i = 1.12 \times 10^{-4}$ M.

NADH faster than the radical cation oxidant and slower than inorganic anion−radical oxidants with $k^{Fe(Cp)_2\bullet+} < k^{ClO_2\bullet} < k^{Br_2\bullet-} < k^{(SCN)_2\bullet-} < k^{I_2\bullet-}$.

Conclusions

The stoichiometry and products of the $ClO_2^\bullet$ oxidation of NADH (determined from UV and ion chromatographic data) show that 1 mol of NADH reacts with 2 mol of $ClO_2^\bullet$ to form 1 mol of NAD^+ and 2 mol of chlorite (ClO_2^-).

The kinetics evaluated by variable-temperature stopped-flow techniques show that the reaction occurs very rapidly even at 3.1 °C. Second-order observed rate constants are obtained from both NADH (k_{obs}^{NADH}, M^{-1} s^{-1}) and $ClO_2^\bullet$ ($k'_{obs}{}^{ClO_2}$, M^{-1} s^{-1}) losses. The $k'_{obs}{}^{ClO_2}/k_{obs}^{NADH}$ ratio of 2.01 represents the stoichiometry of the reaction and supports chromatographic data.

The mechanism in Scheme 2 of a sequential electron transfer with rate-limiting transfer of an electron from NADH to $ClO_2^\bullet$ (k_1, M^{-1} s^{-1}) is suggested on the basis of the detection of ClO_2^- as the single product of $ClO_2^\bullet$ reduction. The formation of NAD^+ and ClO_2^- is observed. Because the rate is not suppressed by the addition of ClO_2^- (meaning irreversibility of the first electron transfer), the observed rate constant k_{obs}^{NADH} of 3.9×10^6 M^{-1} s^{-1} at 24.6 °C is equivalent to k_1. The rate is not affected by variation of pH and buffer concentration. This indicates that acid–base equilibrium is not involved in the rate-limiting step and agrees with the suggested mechanism.

Acknowledgment. This work was supported in part by Purdue University Distinguished Professor Funds for D.W.M. and by a USDA National Needs Fellowship in Food Biosecurity for J.G.A.

IC7019022